



Mechanical Properties and Wear Behaviour of Al 6061 Matrix Composites with Hybrid Reinforcements through Powder Metallurgy Technique

Hussein B. Mohammed¹, Iman M. Naemah¹ and Abdul Jabbar Saad Jomah^{2*}

¹Department of Mechanical Engineering, University of Diyala, 32001 Diyala, Iraq

²Department of Materials Engineering, University of Diyala, 32001 Diyala, Iraq

ARTICLE INFO

Article history:

Received June 8, 2024
Revised November 1, 2024,
Accepted November 16, 2024,
Available online December 1, 2025

Keywords:

Powder metallurgy
Metal matrix composites
Wear rate
Hybrid composites
Mechanical properties

ABSTRACT

Hybrid aluminum composites are frequently used in industrial applications because of their attractive mechanical and tribological properties to weight ratio, such as hardness, strength, and wear resistance. This work investigated the mechanical properties, microstructure, density, and wear behavior of Al-6061 matrix reinforced with different percentages (2 and 4 Wt.% for each Al₂O₃, SiO₂, SiC, and TiO₂) and (2 and 4 Wt.% for each Al₂O₃, TiO₂, and SiC, SiO₂) hybrid composites at 50 μm average size using the powder metallurgy technique. The process of creating a component in net or nearly net shape is known as powder metallurgy. Due to its benefits, including great dimensional control and the avoidance of intermediate machining operations, P/M is one of the fastest-expanding pathways in many industrial applications. According to the results, the optimum hardness and density were 95 HV and 3.1 g/cm³, respectively, for the hybrid composite (Al- 2SiC 2SiO₂) after the sintering operation. The highest hardness was (95HV) at the addition hybrid composite (Al- 2SiC 2SiO₂). Microstructural characterization using optical microscopy shows that the hybrid composite (Al-2%SiC 2%SiO₂) was the best. The SEM photographs of the worn surface of the Al-2%SiC/2%SiO₂ hybrid composite exhibited the least wear losses and grooves. The lowest wear rate was (13*10⁻⁶) at the addition of hybrid composite (Al- 2SiC 2SiO₂) at load (5N).

1. Introduction

In the previous decades, industrial sectors have been driven to improve composite materials so as to increase the overall achievement of marine, automobile, and aircraft component parts [1]. Hybrid composites of aluminum metal matrix are a popular choice to meet industrial needs [2]. The next-generation composites, known as hybrid aluminum matrix composites (HAMC), can replace composites with a single reinforcing and add additional characteristics to enhance the performance of these materials [3, 4]. The proportion of

reinforcement in the composite, the way it interacts chemically with the matrix, the size of the reinforcement's grains, and the manufacturing process all affect its properties [5]. Squeeze casting, powder metallurgy (P/M), semi-solid, stir casting, infiltration, and other processes can all be applied to produce HAMC [6]. HAMC might be regarded as an alternative for traditional materials in several industrial uses because of their desirable properties, enhanced stability at high temperatures, a decreased coefficient of thermal expansion, good capacity to cast, reduced density, more

* Corresponding author.

E-mail address: Abdaljabbar.saad@uodiyala.edu.iq

DOI: [10.24237/djes.2024.18212](https://doi.org/10.24237/djes.2024.18212)

This work is licensed under a [Creative Commons Attribution 4.0 International License](https://creativecommons.org/licenses/by/4.0/).



strength, fewer wear rates, and superior resistance to fatigue [7]. The process of creating a component in net or nearly net shape is known as powder metallurgy. Due to its benefits, including great dimensional control and the avoidance of intermediate machining operations, P/M is one of the fastest-expanding pathways in many industrial applications [8]. In comparison to other manufacturing techniques, powder metallurgy allows for simple control of component density [9]. In order to create hybrid aluminum matrix composites, several studies have examined composites with two reinforcements and above, like SiC particles with SiO₂ or Al₂O₃-reinforced aluminum matrix composites (AMC), with a focus on examining their strength, hardness, wear, and thermal characteristics [10]. When incorporated in metals, silicon carbide (SiC) displays better hardness, higher wear resistance, and higher corrosion resistance [11]. In order to decrease wear, SiC particles can be included with aluminum when making a variety of machine components, such as drive shafts, brake rotors, and drums in automobiles, ventral fins, and fuel access covers in aircrafts. Previous studies have shown that AMC is a superb lightweight multipurpose material with exceptional characteristics that make it a perfect composite for a variety of applications. However, due to its poor resistance against wear and small hardness value, aluminum alloys are required to boost its wear resistance in high-performance tribological uses [12]. Consequently, if these materials were fastened together using bolts or rivets, there is a significant likelihood of oscillation, which in some environmental conditions may result in sliding wear. Since reinforcement of particulates such as SiC, Al₂O₃, and SiO₂ is known to render high specific strength, it can be employed to solve this issue. As a result, metal matrix composites are used to fulfill the demand for materials that are resistant to wear and corrosion [13]. Ceramic particles have been used as reinforcements in numerous powder metallurgy studies using aluminum as the base material. The study of [14] investigated the dry sliding wear behavior of powder metallurgy aluminum matrix composites reinforced with SiC particles. It was discovered

that the addition of SiC particles enhanced the composites' wear resistance and that the wear rate decreased as the volume fraction of SiC particles increased. Meanwhile, [15] found that mechanical properties including tensile strength, yield strength, and hardness are greater compared to the pure Al6063 metals, and that such properties increase by boosting the SiC. SEM was used to analyze the MMC's surface morphology, whereby plowing, microwear, microcrack, fracture, void, and pulling out were observed. An analysis was conducted on the topography and surface texture, in addition to an examination on the MMC's particle distribution. It was found that Al₂O₃, SiC, and TiO₂ are uniformly distributed in the Al6063 matrix. Various morphologies, shapes, and sizes were revealed in the examination of the Al₂O₃, SiC, and TiO₂ in the Al6063 matrix. The MMC's final properties may be affected by the Al₂O₃, SiC, and TiO₂ distribution and dispersion. Next, [16] investigated the fabrication, wear, and mechanical characteristics of Al 6061-silicon carbide-graphite hybrid metal matrix composites. The study discovered that increasing the graphite percentage decreased the composite's wear rate. [17] produced hybrid aluminum matrix composites by P/M with different ratios of Al₂O₃ and SiC. It was found that mechanical properties and wear resistance increase with the addition of ceramic powders (Al₂O₃ and SiC). The study of [18] intended to use the Powder Metallurgy (PM) method to develop Al-matrix composite materials with B4C-SiC and B4C-Y₂O₃ particle reinforcement. Within the composites whereby the employed reinforcement materials are of various particle sizes and ratios, the chosen matrix material was the AA2024 powders. These powders were mixed homogeneously and subsequently compressed under 525 MPa pressure at room temperature. Sintering was then performed on the raw specimens for 45 minutes at various temperatures. Wear tests were performed on the composite materials to determine their hardness and density. This study examined the impact of the multi-particle-size and multi-ratio reinforcement materials that were added to the matrix on wear resistance, density, and hardness at various temperatures. Finally, [19]

investigated the mechanical and microstructure of hybrid aluminum composites reinforced with numerous alumina and silicon carbide particles ratios by using powder metallurgy. The results illustrated that an increase of SiC led to an increase in the compressive strength and hardness of hybrid aluminum composites.

The HAMC will be constructed using the powder metallurgy process as the goal of this study. The application of this research in different engineering industries showed that aluminum 6061 alloy can be strengthened by adding different weight percentages of SiC, Al₂O₃, SiO₂, and TiO₂ particles alone, as well as by adding varying weight percentages of (Al₂O₃+ TiO₂) and (SiC+ SiO₂) hybrid particles. In order to determine the ideal qualities and the ideal addition amount in to the hybrid aluminum composite, the hardness, microstructure, tribological, and density characteristics of the hybrid composite were evaluated as well. In determining the ideal type and quantity of filler particles that can be taken into consideration for a variety of applications, it is important to note that the findings derived would help in designing a new hybrid composite.

2. Experimental work

2-1 Fabrication process

In this search, the fabrication process can be detailed in many steps:

1. Aluminum 6061 powder with a purity level of 97% and typical dimensions of 50 μm was utilized. Table 1 illustrates the chemical composition of aluminum 6061.
2. The Al matrix was reinforced using commercially available Al₂O₃, SiO₂, SiC, and TiO₂ with a 30 μm particle size.
3. The fabrication processes were meticulously carried out by first combining the Al matrix particles with reinforced particle powders at various percentages (2, 4 wt%) and

mechanically grounding them for 2 hours at room temperature using a planetary ball mill (PM 100, Retsch, Haan, Germany) at 300 rpm speed. The weight ratio of the milling balls to the powder was 20:1. For the powder metallurgy process to work, it is crucial to ensure proper mixing.

4. A tubular die with a 10 mm diameter and 30 mm length was discharged with the combined powder.
5. Once done, a binder was added (Mg Stearate) to help prevent particle agglomeration and increase the distribution of reinforcements during ball milling.
6. In this search, using the all-purpose testing device (Instron 3382) on compact powder results in green compacts, which were then pressed for 10 minutes at a pressure of 100 bar in one direction to achieve an initial green density of between 85 and 95%.
7. To avoid oxidation, the sintering process was done in an argon environment at 530 °C for 90 minutes, and the composite specimens shown in Figure 1 were then left to soak in the furnace for 24 hours.
8. In the end-of-production, twelve stander combinations of Al₂O₃, SiO₂, SiC, and TiO₂ were yielded as presented in Table 2.
9. After obtaining the samples, tests were carried out to determine the wear, hardness, microstructure, and density.



Figure 1. Prepared composite specimens.

Table 1: Chemical composition of Al 6061

Element wt.%	Nominal (value) [20]	Measured (value)
Si	0.8	0.542
Fe	0.7	0.561
Cu	0.4	0.321
Mn	0.15	0.112
Mg	1.2	0.933
Cr	0.35	0.211
Ni	0.05	0.0222
Zn	0.25	0.044
Ti	0.15	0.025
Pb	0.02	0.019
V	0.01	0.006
Al	Bal.	Bal.

Table 2: Different compositions of aluminum, (Al₂O₃), (SiO₂), (SiC), and (TiO₂).

Sample	(Wt. %) of various composite	Code
1	98 Al + 2 Al ₂ O ₃	A
2	96 Al + 4 Al ₂ O ₃	B
3	98 Al + 2 TiO ₂	C
4	96 Al + 4 TiO ₂	D
5	98 Al + 2 SiC	E
6	96 Al + 4 SiC	F
7	98 Al + 2 SiO ₂	G
8	96 Al + 4 SiO ₂	H
9	98 Al + 1 Al ₂ O ₃ + 1 TiO ₂	I
10	98 Al + 1 SiC + 1 SiO ₂	J
11	96 Al + 2 Al ₂ O ₃ + 2 TiO ₂	K
12	96 Al + 2 SiC + 2 SiO ₂	L

Note: To avoid repeating the material names and weight fractions throughout the text, we used special codes for the elements (see Table 2).

2.2. Characterization

2.2.1. Micro hardness

A Vickers machine (Leco Microhardness Tester LM248AT) was employed for measuring the microhardness when the complete load was set at 1.96 N with a 15-second dwell duration. Five separate random places were used for the testing, and upon completion, the mean value for each sample's composition was calculated.

2.2.2. Wear test

Utilizing a pin-on-disc wear and friction monitor model (No. DUCOM; TR-20-M100), wear tests were performed under dry sliding conditions in compliance with the ASTM G-99

standard. The machine is made up of a 100-mm-diameter EN32 steel disc with an HRC 58 hardness rating. Cylindrical specimens measuring 10 mm in diameter and 30 mm in height were machined. Wear tests were conducted at normal loads of 5, 10, and 15 N, and the time used was 5 minutes. All tests were conducted in dry conditions at a room temperature of ~ 25 °C, at a fixed distance of 30 mm from the disc's center, and at a speed of 300 rpm, or 1.74 m/s. The disc and the samples were properly cleansed with acetone before and after each test and then dried to prevent contamination. The specimens, with a length of 30 millimeters and diameter of 10 millimeters, were utilized as static pins and manufactured in accordance with ASTM (G99-05) standards. To calculate the wear rate of the specimens, the weight method was applied. Prior to and following the wear test, the specimens were weighed using a sensitive balance of the Denver instrument type (Max-210 g) with 0.0001 gram of precision. Calculation of the wear rate was done using equation (1), after dividing the weight loss (W) by the sliding distance [21].

$$(W.R) = \Delta W / \pi D. N. t \text{ (gm/cm)} \quad (1)$$

where: - (W.R): Wear rate, D: Sliding circle diameter (cm), t: Sliding time (min), N: Disc speed (rpm)

2.2.3. Microstructural characterization

For the evaluation of the microstructural feature, the specimens were prepared by grinding on a variety of polishing papers with grits of 800, 1000, 1200, 1800, 2000, and 2500, and then by alumina slur. They were then cleaned using ultrasonic in acetone and deionized water for 10 minutes, and subsequently dried at 100°C for 1 hour. The microstructure and abraded surface of the composites were characterized using optical microscopes of the Optika-Italy and SEMs of the FEI 9922650 type with high resolution.

2.2.4. Density characterization

The Archimedes principle was used to determine the density of all the composite materials. The theoretical composite density was computed utilizing the rule of mixing equations, and the composite density was measured by the water displacement method.

3. The results

3.1. Micro hardness

Figures 2 and 3 show the results of the microhardness test for the specimens reinforced by 2 and 4 weight percent of each A, B, C, D, E, F, G, and H. The results show that pure aluminum 6061 exhibits the lowest value of microhardness in comparison to specimens reinforced by (2 and 4 Wt.% for each A, B, C, D, E, F, G, and H), while the other specimens do not display this effect. These numbers show that adding reinforcement particles increases the composite material's hardness, which also rises as the reinforcement particles' weight percentage increases. With 4% more SiC particles added, the hardest material is 85 HV.

The microhardness test results for the specimens reinforced by (2 and 4 weight percent) of each hybrid composite of (I, J, K) and (L) are shown in Figure 4. The hybrid

composites' mechanical characteristics are influenced by several factors, including the reinforcing materials and the matrix's interaction, the microstructure, the sintering temperature, as well as the volume fraction of the reinforcing elements [22]. As seen in Figure 4, the hardness of the hybrid composite rises as more hybrid reinforcement is added to the metal and as the ratio of hybrid powder in the composite increases. The Al matrix had a 95 HV hardness when 4% of L particles were introduced. The development of the composite's hardening may be attributed to a variety of factors, including the higher stiffness of the SiC and SiO₂ powders, the strong interfacial adhesion between aluminum and SiC, as well as the significant increase in density. Additionally, the addition of ceramic particles may have halted the migration of dislocations, limiting the composite's ability to deform, which is one reason for the rise in microhardness in the HAMC. The microhardness of the composite grew dramatically when the volume fraction of SiC was increased, whereas the hardness of the composite only slightly rose when the weight percentage of silicon oxide was increased. From the figure, the hybrid filer (4% of L) has higher hardness.

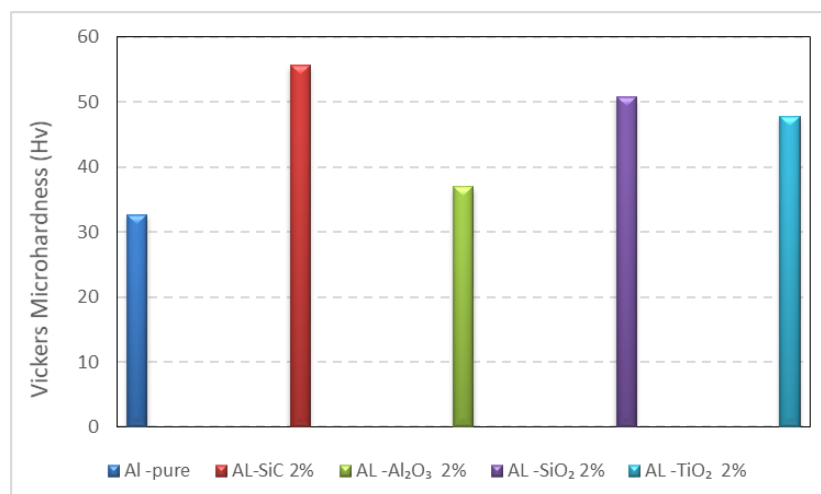


Figure 2. Illustrates the micro hardness of aluminum and composite at wt.2 % of (SiC, Al₂O₃, SiO₂, & TiO₂).

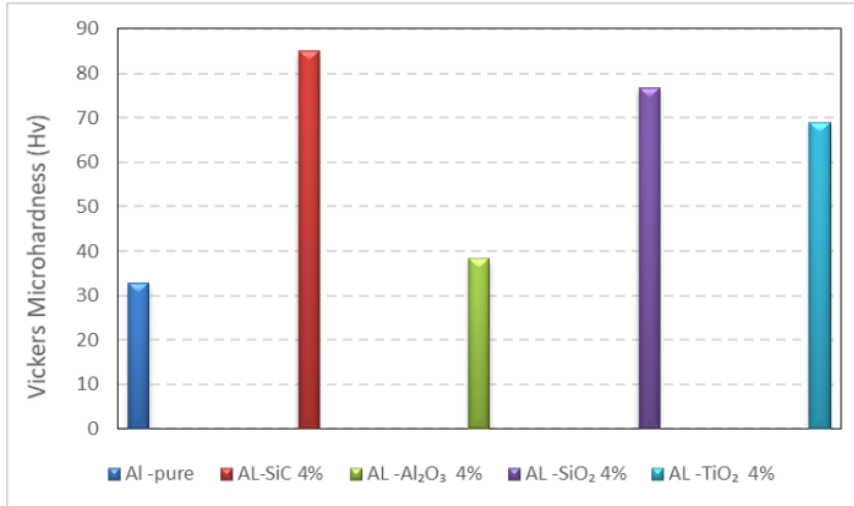


Figure 3. Illustrates the micro hardness of aluminum and composite at wt.4% of (SiC, Al₂O₃, SiO₂, & TiO₂)

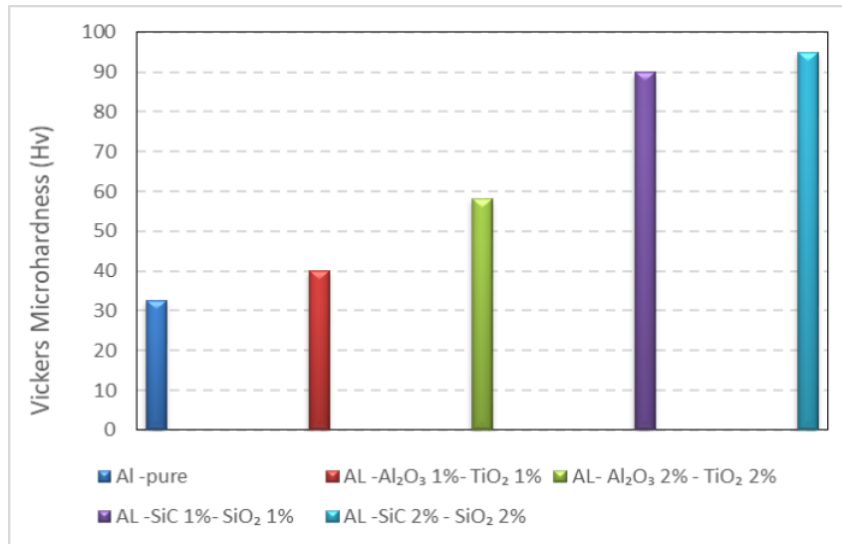


Figure 4. Micro hardness of aluminum and hybrid composite at 2wt. % and 4wt. % of (Al₂O₃+ TiO₂ and SiC+ SiO₂)

3.2 Wear test

3.2.1. Effect of particles content on wear rate

Figures 5, 6, and 7 show the relationship between the volume ratio of composites made of (A, B, C, D, E, F, G, and H) and (I, J, K) and (L) hybrid composites. It is clear that by increasing the reinforcing percentage from 2 weight percent to 4 weight percent following all the applied loads' increment, a decrease occurs in the wear rate. Increasing the hardness of the composite, as illustrated in Figures 2 and 3, led to a decrease in the wear rate. Because of the tougher particles and the force that holds them

to the Al matrix, a higher wear resistance is observed in the composite. Archard's law [23] can be used to predict this behavior:

$$W = K (N.S./C.H.) \tag{2}$$

Where W, N, K, S, C, and H stand for, respectively, wear loss, normal applied load, wear constant, sliding distance, geometrical factor of the microstructure, and composite hardness.

The significant increase in density, as seen in Figure 8, as a result of the higher reinforcing percentage, resulted in a reduction in wear rate. This reduction was also caused by a tight link between the composite particles, which

rendered it difficult for them to dislocate out of place when sliding.

The results show that the hybrid composite (L) at 5N load had the lowest wear rate (13×10^{-6}), which increased as the applied load rose.

3.2.2. Effect of applied loads on wear rate

The wear rate variations for the single and hybrid composites under various applied loads for all reinforcing particle weight percentages

are shown in Figures 5, 6, and 7. It is evident that as the applied stresses increased, the wear resistance dropped. Since the contact and friction between the tribo surfaces amplified and contributed to the quick deformation of the single and hybrid composites because of compressive and frictional forces that predominated in dry sliding, it follows that the wear rate must be improved by boosting the loads, as reported by Archard's law [24].

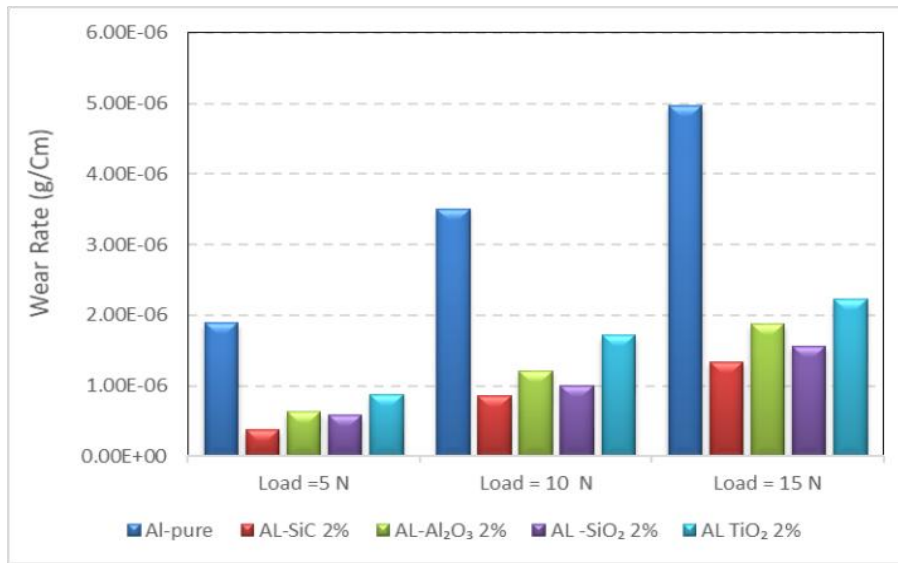


Figure 5. Wear rate of aluminium and composite at wt. 2 % of (SiC, Al₂O₃, SiO₂, & TiO₂) at various loads

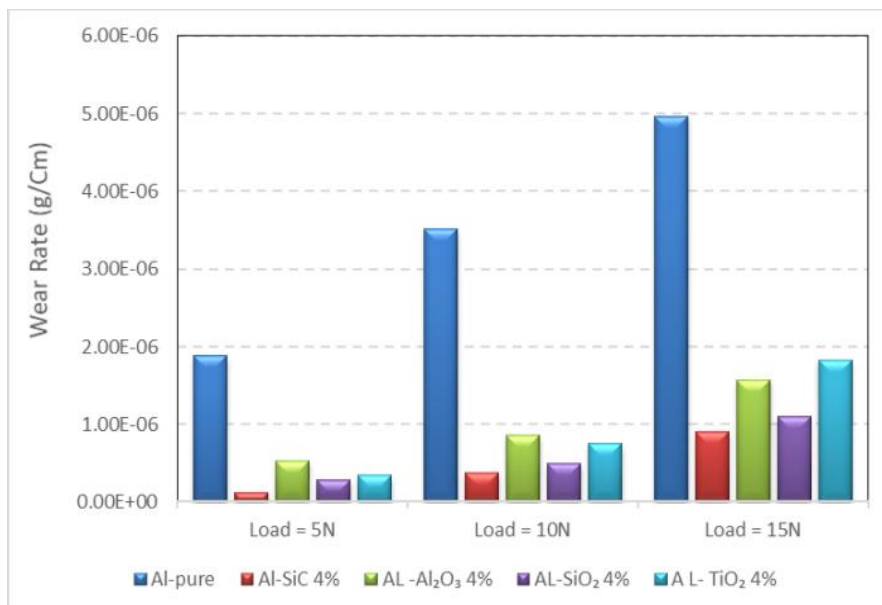


Figure 6. Wear rate of aluminium and composite at wt. 4 % of (SiC, Al₂O₃, SiO₂, & TiO₂) at various loads

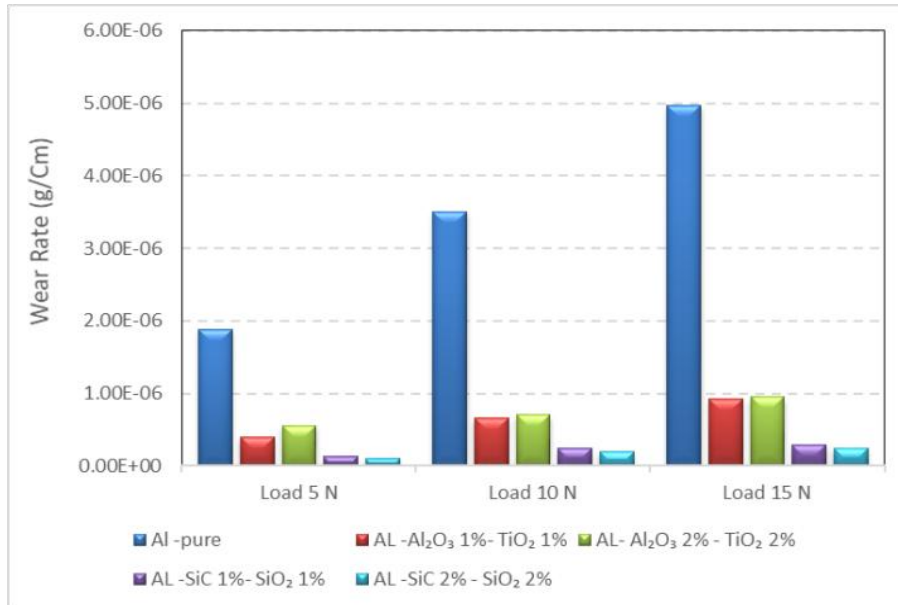


Figure 7. Wear rate of aluminum and hybrid composite at 2wt. % and 4wt. %. (SiC, Al₂O₃, SiO₂, & TiO₂) at various loads

3.3 Density measurements

Figure 8 shows the density of the twelve samples at various compositions, both before and after sintering. In this search, we used Archimedes' method to calculate the density of all single composites and hybrids. The theoretical composite density was computed utilizing the rule of mixing equations, whilst the composites' density was determined using the

water-displacement approach [25]. Comparing the composite density results to the theoretical density values demonstrates that the samples are fully dense. That composites have a higher density than their basic matrix (2.7 g/cm³ for aluminum 6061), and that the density of the composites rises as the proportion of flier content in the composites increases. Figure 8 shows that the higher density at (L) was 3.1 g/cm² and increased after sintering.

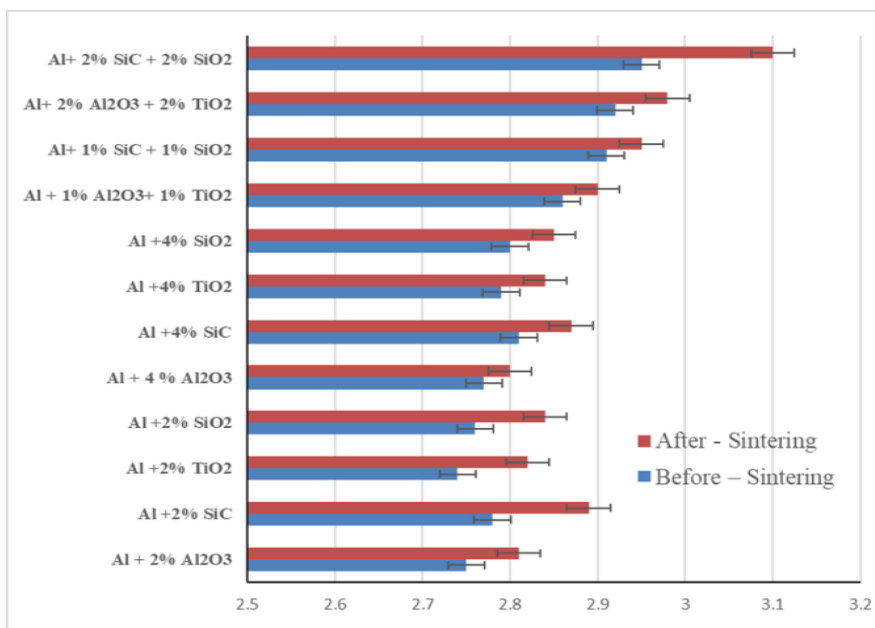


Figure 8. Change of density for single and hybrid composites, after and before sintering

3.4 Microstructural evaluation

From the hardness and wear tests, the best mechanical properties are at an additional 4% wt. for the single and hybrid composite for F and L, whilst B and K demonstrated the minimum properties at the same percentage. The optical microscopy images for Al6061 single and hybrid composites are at 4 weight percent. B, F, K, and L are all depicted in Figure 9 in the order listed.

The Al_2O_3 particles are distributed uniformly throughout the Al matrix, as seen in Figure 9a. F particles are depicted in Figure 9b as a gray element that is spread very equally throughout the Al base metal. The microstructure of Al was altered by the addition of F, improving the mechanical characteristics. Figure 9c shows K particles; it was observed in the microstructure that B and C's distributions were largely homogeneous and sometimes non-homogeneous, and that the structure was largely non-porous.

Figure 9d depicts the hybrid composite (L); the image shows an even distribution of SiO_2 particles throughout the base alloy matrix and a consistent mixture of Al 6061, SiC, and SiO_2 . As a more compact structure was obtained, the image with the smallest black zone depicts the specimen's minimum level of porosity creation. This distribution resulted in an excellent microstructure and strong mechanical properties.

3.5. Wear surface assessment

From the hardness and wear tests, the best mechanical properties are at an additional 4% wt. for the single and hybrid composite for F and L, whilst B and K demonstrated the minimum properties at the same percentage. The optical microscopy images for Al6061 single and hybrid composites are at 4 weight percent. B, F, K, and L are all depicted in Figure 9 in the order listed. The Al_2O_3 particles are distributed uniformly throughout the Al matrix, as seen in Figure 10a. F particles are depicted in Figure 10b as a gray element that is spread very equally throughout the Al base metal. The microstructure of Al was altered by the addition of F, improving the mechanical characteristics. Figure 10c shows the K particles; it was observed in the microstructure that B and C' distributions were largely homogeneous and sometimes non-homogeneous, and that the structure was largely non-porous. Figure 10d depicts the hybrid composite (L); the image shows an even distribution of SiO_2 particles throughout the base alloy matrix and a consistent mixture of Al 6061, SiC, and SiO_2 . As a more compact structure was obtained, the image with the smallest black zone depicts the specimen's minimum.

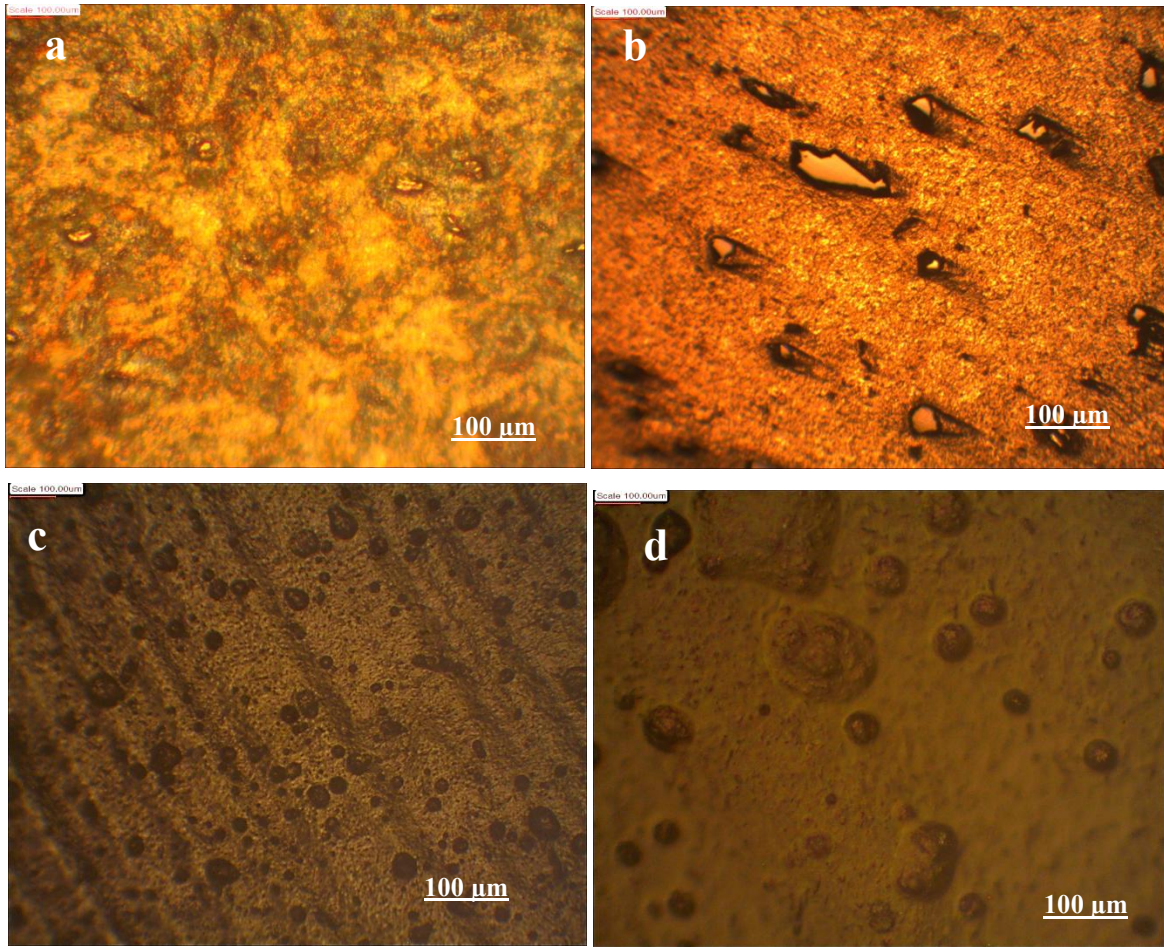


Figure 9. Optical microscopy for single and hybrid composites at 4wt. %.: (a) Al₂O₃, (b) SiC, (c) Al₂O₃+ TiO₂, and (d) SiC+ SiO₂.

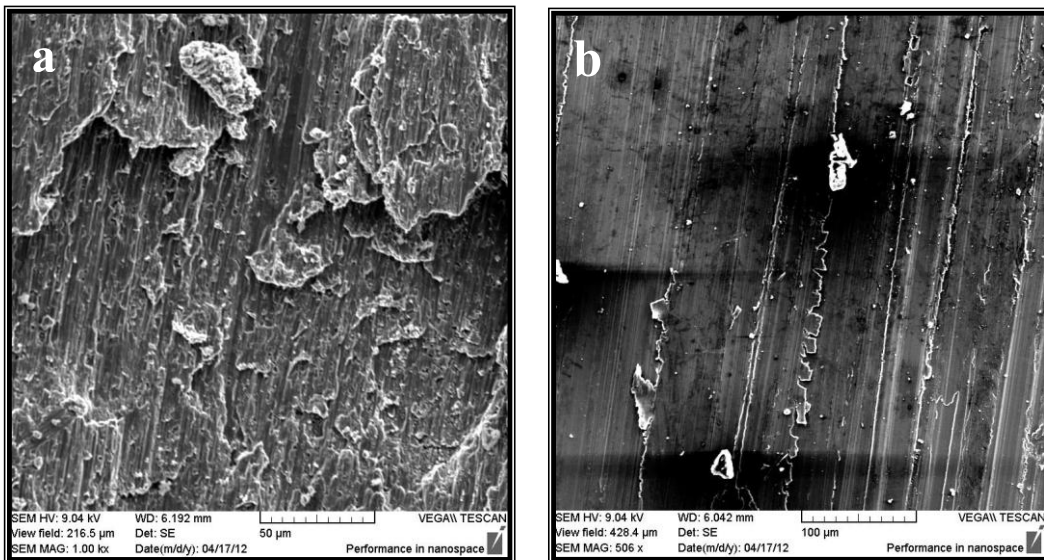




Figure 10. SEM photographs of worn surfaces for single and hybrid composites at 4wt. %.: (a) Al_2O_3 , (b) SiC, (c) $\text{Al}_2\text{O}_3 + \text{TiO}_2$, and (d) $\text{SiC} + \text{SiO}_2$ at an applied load of 5N

4. Conclusions

Novel and optimized hybrid composites were successfully prepared to improve mechanical and tribological in order to identify the optimum amount of filler without mechanical degradation, using low-cost powder metallurgy method. The following conclusions were made throughout this work:

1. The hybrid composite (Al- 2SiC+ 2SiO₂) can obtain a higher microhardness value of 95 HV.
2. The lowest wear rate is (13×10^{-6}) at the addition of hybrid composite (Al-2SiC+2SiO₂) at load (5N) and increases with increased applied load.
3. The density of composites increases as the proportion of filler content rises; the hybrid composite (Al-2%SiC+2%SiO₂) has the highest density after sintering at 3.1 g/cm³.
4. Microstructural characterization using optical microscopy shows that the hybrid composite (Al-2%SiC+2%SiO₂) is the best as there was uniform mixture, minimum porosity formation, and good distribution of particles.

5. The SEM photographs of the Al-2%SiC+2%SiO₂ hybrid composite's worn surface exhibit the least damage and grooves.

References

- [1] Qu, X.-H.; Zhang, L.; Mao, W.; Ren, S.-B. "Review of metal matrix composites with high thermal conductivity for thermal management applications" *Mater. Int.* 2011, 21, 189–197.
- [2] Ahamad, N.; Mohammad, A.; Sadasivuni, K.K.; Gupta, P. "Structural and mechanical characterization of stir cast Al–Al₂O₃–TiO₂ hybrid metal matrix composites" *J. Compos. Mater.* 2020, 54, 2985–2997.
- [3] Manikandan, R.; Arjunan, T. "Studies on micro structural characteristics, mechanical and tribological behaviours of boron carbide and cow dung ash reinforced aluminium (Al 7075) hybrid metal matrix composite" *Compos. Part B Eng.* 2020, 183, 107668.
- [4] A.J.S. Jomah, A.F. Hasan, W. Al Azzawi, "Microstructure and Mechanical Properties of Friction Crush Welded 1145 Aluminum Sheets with Flanged Edges", *Materials Research* 26 (2023) e20220419. DOI: <https://doi.org/10.1590/1980-5373-MR-2022-0419>
- [5] Nayim, S.T.I.; Hasan, M.Z.; Seth, P.P.; Gupta, P.; Thakur, S.; Kumar, D.; Jamwal, A. "Effect of CNT and TiC hybrid reinforcement on the micro-mechano-tribo behavior of aluminium matrix composites" *Mater. Today Proc.* 2020, 21, 1421–1424.

- [6] Kavimani, V.; Prakash, K.S.; Thankachan, T. "Experimental investigations on wear and friction behaviour of SiC@ r-GO reinforced Mg matrix composites produced through solvent-based powder metallurgy" *Compos. Part B Eng.* 2019, 162, 508–521.
- [7] Sharma, S.; Nanda, T.; Pandey, O. "Effect of particle size on dry sliding wear behavior of sillimanite reinforced aluminium matrix composites" *Ceram. Int.* 2018, 44, 104–114.
- [8] M. Reihanian, S. R. Asadullahpour, S. Hajarpour, and KGheisari, "Application of neural network and genetic algorithm to powder metallurgy of pure iron" *Materials and Design*, vol. 32, no. 6, pp. 3183–3188, 2011.
- [9] N. Nandakumar and R. Vivekanandan, "Experimental investigation of corrosion characteristics on Al6063 hybrid metal matrix composites" in *Proceedings of the International Conference on Advances in Materials, Manufacturing and Applications*, p. 27, Bengaluru, India, April 2015.
- [10] Prakash, C.; Singh, S.; Sharma, S.; Garg, H.; Singh, J.; Kumar, H.; Singh, G. "Fabrication of aluminium carbon nano tube silicon carbide particles-based hybrid nano-composite by spark plasma sintering" *Mater. Today Proc.* 2020, 21, 1637–1642.
- [11] L. Shi, C. Sun, P. Gao, F. Zhou, and W. Liu "Mechanical properties and wear and corrosion resistance of electrodeposited Ni-Co/SiC nanocomposite coating" *Applied Surface Science*, vol. 252, no. 10, pp. 3591–3599, 2006.
- [12] Satyanarayana, T.; Rao, P.S.; Krishna, M.G. "Influence of wear parameters on friction performance of A356 aluminum-graphite/graphite particles reinforced metal matrix hybrid composites" *Heliyon* 2019, 5, e01770.
- [13] Fenghong, C.; Chang, C.; Zhenyu, W.; Muthuramalingam, T.; Anbuechhiyan, G. "Effects of silicon carbide and tungsten carbide in Aluminium metal matrix composites" *Silicon* 2019, 11, 2625–2632.
- [14] R. Ganesh, Ram Subbiah & K. Chandrasekaran "Dry Sliding Wear Behavior of Powder Metallurgy Aluminium Matrix Composite" *Materials Today: Proceedings*, 2, 2015, 1441 – 1449.
- [15] M.B.A. Shuvho, M.A. Chowdhury, M. Kchaouc, A. Rahmanb, M.A. Islamb "Surface characterization and mechanical behavior of aluminum based metal matrix composite reinforced with nano Al₂O₃, SiC, TiO₂ particles" *Chemical Data Collections*, 28, 2020, 100442.
- [16] P. S. Shivakumar Gouda & G.B. Veeresh Kumar "Fabrication, mechanical and wear properties of Aluminum (Al6061)-silicon carbide-graphite Hybrid Metal Matrix Composites" *Frattura ed Integrità Strutturale*, 62, 2022, 134-149.
- [17] L. Natrayan, M. Santhosh, R. Mohanraj, and R. Hariharan, "Mechanical and Tribological Behaviour of Al₂O₃&SiC Reinforced Aluminium Composites Fabricated via Powder Metallurgy," *IOP Conference Series: Materials Science and Engineering*, vol. 561, no. 1, Article ID 012038, 2019.
- [18] Halit Doğan, Yılmaz Mutlu, "Production of AA2024-Matrix B₄C-SiC- and B₄C-Y₂O₃-Particle-Reinforced Composites by Powder Metallurgy and Investigation of Their Mechanical Properties", *Celal Bayar University Journal of Science*, Vol. 18, Issue 3, 2022, p 321-330, Doi: 10.18466/cbayarfbe.1130031.
- [19] M. S. Kumar, L. Natrayan, R. D. Hemanth, K. Annamalai, and E. Karthick, *Experimental investigations on mechanical and microstructural properties of Al₂O₃/SiC reinforced hybrid metal matrix composite*, IOP Publishing, Bristol, U.K.
- [20] The Aluminum Association (1994) and Davis (1993).
- [21] Sanders B. R. and Weintraub T. L., "Metal Handbook Mechanical Testing" Vol. 8, 9th ed. USA, 1985.
- [22] Bisht, A.; Kumar, V.; Li, L.H.; Chen, Y.; Agarwal, A.; Lahiri, D., "Effect of warm rolling and annealing on the mechanical properties of aluminum composite reinforced with boron nitride nanotubes", *Mater. Sci. Eng. A* 2018, 710, 366–373.
- [23] Mahdi FM, Razooqi RN, Irhayyim SS, "The influence of graphite content and milling time on hardness, compressive strength and wear volume of copper-graphite composites prepared via powder metallurgy", *Tikrit J Eng Sci*, 24, 2017 47–54.
- [24] Saif S. Irhayyim, Hashim Sh. Hammood and Anmar D. Mahdi, "Mechanical and wear properties of hybrid aluminum matrix composite reinforced with graphite and nano MgO particles prepared by powder metallurgy technique", *AIMS Materials Science*, 2020, 7(1), 103–115.
- [25] Tabonah, T.M.K.; Akkas, M.; Islak, S., "Microstructure, Wear and Corrosion Properties of NiB-TiC Composite Materials Produced By Powder Metallurgy Method", *Sci. Sinter.* 2019, 51, 327–338.

